The Hong Kong Institution of Engineers Transactions, Vol 18, No 4, pp32-38
Paper A017-201104; Received 1 April 2011; Accepted 29 June 2011

SHORTLISTED PAPER

Impedance Network for Power Optimisation in Piezoelectric Energy Harvesting Systems

Distributed wireless sensor network would be autonomous by scavenging energy from the ambience. The piezoelectric materials provide one of the promising transduction mechanisms for harvesting the ambient vibration energy. In the piezoelectric energy harvesting (PEH) systems, even it was claimed that the harvested power can be optimised with the impedance matching theory, several fundamental issues were still not thoroughly investigated or even misunderstood. Retrospecting to the origin of the impedance matching theory, the equivalent impedance network for PEH systems is proposed in this paper with emphases on its scope, as well as the definition, available range, and composition of the electrical part equivalent impedance. Due to the distinctions between the equivalent impedance network of the PEH systems and the unconstrained impedance network, the conventional complex conjugate and resistive impedance matching theories can no longer be directly used for the harvested power optimisation. Instead, constrained impedance matching should be adopted. Experimental results obtained from a base excited PEH device show that the harvested power can be well predicted with the equivalent impedance network. The limitation on the electrical part equivalent impedance in the specific PEH system is also discussed with the matching index defined in this paper.

Keywords: *Piezoelectric, Energy Harvesting, Impedance Matching, Power Optimisation*

LIANG Junrui*
Department of Mechanical and Automation Engineering, The Chinese University of Hong Kong

LIAO Wei Hsin
Department of Mechanical and Automation Engineering, The Chinese University of Hong Kong

** The first author who is at the age of 35 or below on the closing date of submission*

Introduction

The technologies of energy harvesting (also known as power harvesting and energy scavenging) provide the possibility that ambient energy in different forms is converted, captured and stored (usually in electrical energy). The most investigated ambient energy sources include solar energy, wind energy, kinetic energy, thermal energy, and RF radiation (Cook-Chennault *et al.*, 2008; Hudak *et al.*, 2008). The scattering nature of these ambient sources makes the energy harvesting systems different from the conventional centralised power plants. These energy harvesting systems are more suitable to be equipped as the power supplies in low power wireless autonomous devices. Ubiquitously deployed wireless sensor networks (WSNs) and low power portable electronics are the most potential applications, which might be benefited from the development of energy harvesting technologies.

Piezoelectric energy harvesting (PEH) systems scavenge the ambient vibration energy using the piezoelectric transducer, which is the simplest transducer to fabricate among the commonly used electromechanical transducers. Therefore, the PEH systems are particularly suitable for implementation in microsystems (Beeby *et al.*, 2006). From the application point of view, a complete piezoelectric energy harvesting system can be broken down into six parts, as illustrated in Fig 1: excitation and mechanical transformer fully in mechanical domain; piezoelectric transducer in half mechanical and half electrical domain; interface circuit, energy storage, and dc load fully in electrical domain. The piezoelectric transducer is the key component in the harvesting system. It links the mechanical and electrical domains with its piezoelectric effect, which produces electric potential when stress is applied.

For example, Fig 2 shows the configuration of a base excited PEH device. Referring to the block diagram in Fig 1, the base acceleration $\ddot{y}(t)$, second derivative of the base displacement y(t) with respect to time, is the mechanical excitation. Through mechanical transformation mechanisms (the bending cantilever with end mass), the base vibration is transformed into alternating longitudinal deformation of the piezoelectric patch. Due to the piezoelectric effect, a charge movement is then induced through the element. As far as the end devices are usually digital electronics, which require dc voltage power supply, an interface circuit is followed for ac-dc rectification. The device in Fig 2 adopts a bridge rectifier for rectification. It is the most standard interface circuit, which is called standard energy harvesting (SEH) interface. The filter capacitor C_{rect}

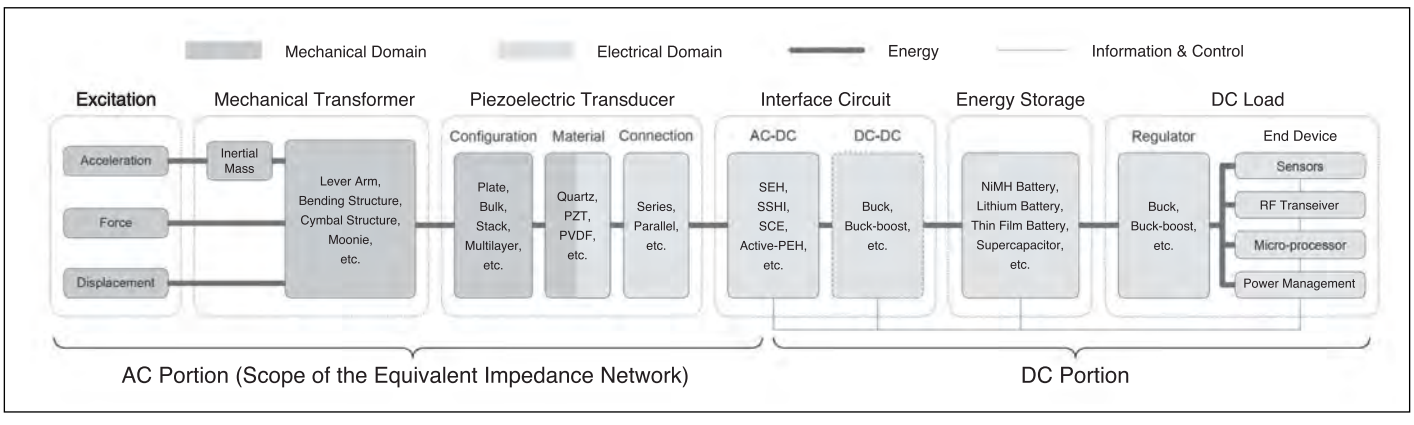

Figure 1 – Block Diagram of a PEH System

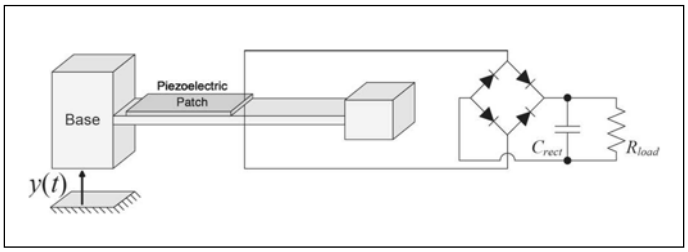

Figure 2 – A Base Excited PEH Device

Component	Corresponding Block
Base Acceleration $\ddot{y}(t)$	Excitation
Bending Cantilever with End Mass	Mechanical Transformer
Piezoelectric Patch	Piezoelectric Transducer
Bridge Rectifier	Interface Circuit
Filter Capacitor C_{rect}	Energy Storage
Resistor R_{load}	DC Load

Table 1 – Components in the Base Excited PEH Device and Their Corresponding Blocks

acts as the energy storage, while R_{load} represents the dc load. Table 1 summarises the relation between the components in the base excited PEH example and the blocks in the block diagram.

Harvested power optimisation is one of the key issues in the research of PEH. In the conventional power systems, the maximum power transfer theorem is regarded as the criterion for load power optimisation, ie, the load power can be maximised when the load impedance matches the source impedance. Yet, for the PEH systems, which have a coupling effect between the parameter distributed mechanical structure and the nonlinear harvesting circuit, the power optimisation is not so straightforward. Conflicting viewpoints were found in the previous literature, which discussed the utilisation of impedance matching for the power optimisation in the PEH systems. Rodig *et al.* (2010), Uchino and Ishii (2010), Kim *et al.* (2007), and Stephen (2006) divided the harvested power optimisation process into two stages: mechanical impedance matching and electrical impedance matching; the interaction between the mechanical and electrical parts of the PEH systems was not truly reflected. Brufau-Penella and Puig-Vidal (2009), Scruggs (2010), and Kong *et al.* (2010) considered the impedance matching from the system level by modelling the mechanical part into equivalent circuit. Yet, Brufau-Penella and Puig-Vidal (2009) and Scruggs (2010) have not considered the effect of real (nonlinear) harvesting circuits; they assumed that a harvesting circuit can be equalised to linear load whose impedance can be arbitrarily set. On the other hand, Kong *et al.* (2010) regarded the effect of a real harvesting circuit as resistive impedance; they proposed a discontinuous conduction mode (DCM) buck-boost converter for the resistive impedance matching purpose.

In all of the above-mentioned literature, it was claimed that the impedance matching theory can be used for harvested power optimisation in PEH systems. Nevertheless, four fundamental issues are still contradicting or ambiguous:

1) The scope of the equivalent impedance network;
2) The definition of the equivalent impedance of a real harvesting circuit;
3) The attainable range of the equivalent impedance of a harvesting circuit;
4) The detailed composition of the equivalent impedance in a harvesting circuit.

Without considering these issues, the impedance matching for the harvested power optimisation in PEH systems could be misunderstood. On the other hand, conflicts were also found in utilising the impedance matching theory for power optimisation in the electromagnetic energy harvesting systems (Stephen, 2006).

In this paper, the above-mentioned four issues are clarified, so that the equivalent impedance network of a whole PEH system can be obtained. Based on the new understanding, it will be shown that the conventional complex conjugate and resistive impedance matching laws are not directly applicable for a PEH system with real harvesting circuit. The difference between the impedance matching in the conventional impedance networks and that in the PEH systems will be comprehensively discussed in the following sections.

Equivalent Impedance Network

As an electromechanical system, a PEH system is composed of two parts, the mechanical and electrical parts. Before utilising the impedance matching technique to optimise the harvested power in the PEH systems, it is necessary to specify the scope of the equivalent impedance network, which can uniformly describe the dynamics of both the mechanical and electrical parts in the PEH systems. The impedances of all components in a real PEH system as well as their constraints should be well studied. The source and load impedances should also be identified from the equivalent impedance network. Nevertheless, some or all of these considerations were lacked in the previous literature about impedance matching for energy harvesting systems (Kim *et al.*, 2007; Stephen, 2006; Brufau-Penella and Puig-Vidal, 2009; Scruggs, 2010; Kong *et al.*, 2010; Stephen, 2006).

Scope of the Equivalent Impedance Network

Rodig *et al.* (2010), Uchino and Ishii (2010), Kim *et al.* (2007), and Stephen (2006) divided the system into two separated impedance networks, the mechanical and electrical networks. The mechanical domain matching deals with the pure mechanical network, so that the power delivered to the transducer can be maximised in the mechanical domain. The electrical domain matching deals with the pure electrical network, so that the harvested power can be maximised in the electrical domain. But this proposition is only valid for the weakly coupled systems, since the interaction between the mechanical and electrical parts is not included in these models.

A more general model should combine the two separated impedance networks into one, so that the overall dynamics of a PEH system can be taken into consideration. Referring to the block diagram shown in Fig 1, a PEH system is divided into ac and dc portions. But since an impedance network cannot be ac and dc at the same time, the loading effect of the dc portion is reflected by different rectified voltage in the ac-dc conversion. Taking the input impedance of the interface circuit as a function of the rectified voltage, the ac portion of the PEH system can be fully converted into a pure ac impedance network. Such kind of the equivalent ac impedance network was used by Brufau-Penella and Puig-Vidal (2009) and Scruggs (2010), but the actual input impedance of real interface circuits was not considered in their studies. The real interface circuit was taken into consideration by Kong *et al.* (2010), but the input impedance of the ac-dc stage was confused with that of the dc-dc stage.

Definition of the Electrical Part Equivalent Impedance

Conventionally, the concept of impedance is usually used for lumped and linear systems to show the magnitude and phase relations between the across and through variables. In a PEH system, the mechanical part is parameter distributed rather than lumped structure; the harvesting circuit is nonlinear. But both the dynamics of the mechanical and electrical parts can be approximated by their equivalent impedance.

With the mechanical to electrical analogy, each mode of the structure can be equivalently represented by an RLC branch in the electrical domain. The corresponding resistance, inductance, and capacitance values can be obtained by experimental identification (Guan and Liao, 2009), analytical method (Elvin and Elvin, 2009), or numerical analysis (Yang and Tang, 2009). When working under a specific vibration mode, Fig 3 shows the equivalent circuit of the base excited PEH device as in

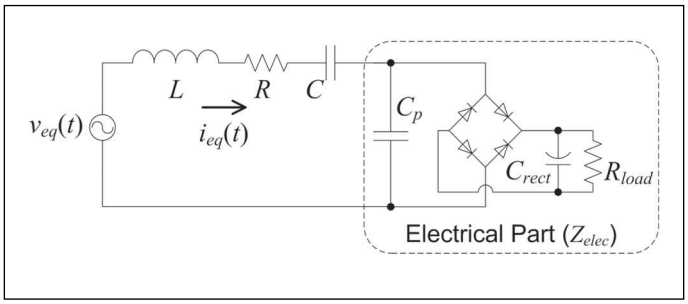

Figure 3 – Equivalent Circuit of a Base Excited PEH Device

Fig 2. The voltage source $v_{eq}(t)$ is proportional to the base acceleration $\ddot{y}(t)$; the inductance L, resistance R, and capacitance C correspond to the effective mechanical mass, damping and short circuit stiffness.

From the equivalent circuit shown in Fig 3, the electrical part of the system is composed of the clamped capacitance C_p and the harvesting interface circuit. In the previous literature, the harvesting interface circuit was regarded as equivalent to pure resistance (Kong *et al.*, 2010) or resistance plus inductance (Brufau-Penella and Puig-Vidal, 2009). Yet, the definition on the equivalent impedance of a nonlinear harvesting circuit was not given. Given that the impedance of an electrical component reflects the magnitude and phase relations between the voltage across and current through this component, it is better to look for the definition from the voltage and current waveforms.

Assuming that the influence of higher-order harmonics caused by the harvesting circuit is much smaller than that of the fundamental harmonic, the equivalent current under a specific harmonic excitation is regarded as perfect sine wave:

$$i_{eq}(t) = I_0 \sin(\omega t) \tag{1}$$

where I_0 and ω are the magnitude and frequency of $i_{eq}(t)$. With the SEH interface circuit, the voltage across the piezoelectric element can be described by the following piecewise equation:

$$v_p(t) = \begin{cases} V_{oc}[1 - \cos(\omega t)] - V_{rect}, & 0 \le \omega t < \theta; \\ V_{rect}, & \theta \le \omega t < \pi; \\ V_{rect} - V_{oc}[1 + \cos(\omega t)], & \pi \le \omega t < \pi + \theta; \\ -V_{rect}, & \pi + \theta \le \omega t < 2\pi. \end{cases} \tag{2}$$

V_{oc} is the magnitude of the open circuit voltage:

$$V_{oc} = \frac{I_0}{\omega C_p} \tag{3}$$

θ corresponds to the rectifier blocked interval in a half cycle (as illustrated in Fig 4); V_{rect} is the rectified voltage. θ and V_{rect} are related by:

$$\cos\theta = 1 - 2\tilde{V}_{rect} \tag{4}$$

where $\tilde{V}_{rect}$ is the non-dimensional rectified voltage defined as:

$$\tilde{V}_{rect} = \frac{V_{rect}}{V_{oc}} \tag{5}$$

The rectified voltage V_{rect} is the sum of V_{store} (the voltage across C_{rect}) and V_F (the forward voltage drop of the bridge rectifier).

Fig 4 shows the waveforms of the voltage across and current through the electrical part. The impedance of the electrical part cannot be obtained with i_{eq} and v_p, since v_p is not sinusoidal. The closest approximation is to substitute v_p with its fundamental harmonic:

$$v_{p,F}(t) = \frac{I_0}{2\pi\omega C_p}\{[\sin(2\theta) - 2\theta]\cos(\omega t) + 2\sin^2\theta \sin(\omega t)\} \tag{6}$$

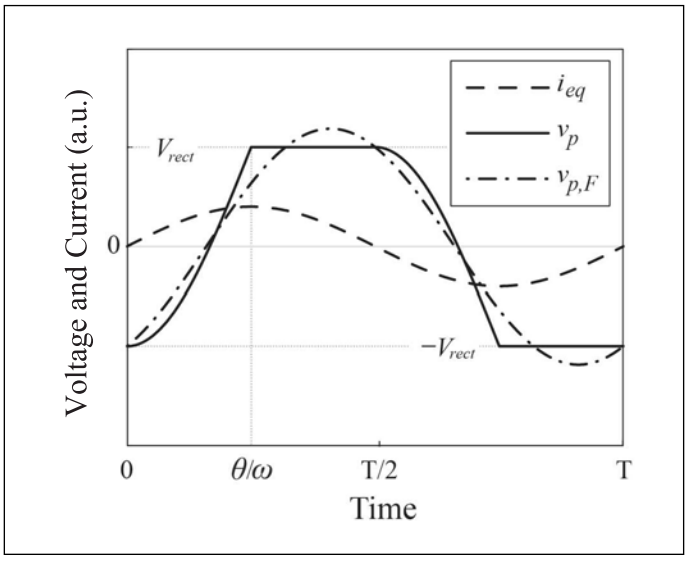

Figure 4 – Characteristic Voltage and Current Waveforms in SEH

The waveform of $v_{p,F}$ is also shown in Fig 4. The equivalent impedance of the electrical part is obtained with the Fourier transform of Eqn (1) and Eqn (6):

$$Z_{elec}(j\omega) = \frac{V_{p,F}(j\omega)}{I_{eq}(j\omega)} = \frac{I}{\pi\omega C_p}[\sin^2\theta + j(\sin\theta\cos\theta - \theta)] \tag{7}$$

When the excitation frequency ω is determined, $\tilde{Z}_{elec}$ is independent of the voltage source, but merely depends on θ or $\tilde{V}_{rect}$.

Range of the Electrical Part Equivalent Impedance

Eqn (7) gives the expression of the electrical part equivalent impedance with the SEH interface circuit. Since the range of θ is confined in $[0, \pi]$, the value of Z_{elec} should be constrained, rather than can be arbitrarily set.

In some studies, the performance of SEH interface circuit was compared with that of the resistive shunt damping (RSD), ie only a resistor is connected as the interface circuit. Fig 5 illustrates the electrical part equivalent impedance in these two cases on the non-dimensional complex impedance plane. From Fig 5, the equivalent impedance in SEH can be changed along the solid curve by adapting the rectified voltage; the equivalent impedance in RSD can be changed along the dash curve by adapting the value of the connected resistor. The dynamics in the two cases are different; their intersection has only two points: (0, 0) and (0, -1), which correspond to the short circuit and open circuit conditions, respectively.

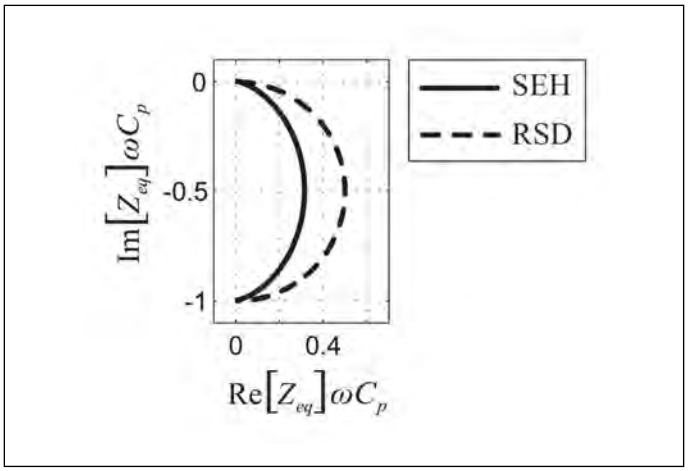

Figure 5 – Equivalent Impedance of SEH and RSD

Detailed Composition of the Electrical Part Equivalent Impedance

The definition and range of the electrical part equivalent impedance were studied, but it is still unable to specify the optimisation task. The power delivered to the electrical part or harvesting circuit is only the power that is extracted from the PEH system, rather than the power that is harvested. The subtle relation between extracted and harvested power can be explained by studying the energy flow in the PEH system.

The energy flow chart shown in Fig 6 gives an intuitive understanding on the energy relation in the PEH system. Liang and Liao (2011) provided the detailed explanation to the energy flow chart. In the electrical domain, there are three possible destinations for the input energy:

1) being converted into thermal energy (branch G), ie dissipated;
2) being stored in energy storage devices and/or used to power the end device (branch I), ie harvested;
3) returning to the mechanical domain (branch J).

Within these three branches of energy flow, both the first and second branches extract power from the system, but only the second one, the harvesting branch, is the targeted branch for optimisation, as illustrated in Fig 6. This detail cannot be shown with the purely electrical part impedance Z_{elec}. In order to identify the targeted branch, Z_{elec} should be further divided into three components: vibratory component X_E, harvesting component R_h, and dissipative component R_d. Because the total extracted power is composed of the harvested and dissipated portions, the sum of R_h and R_d corresponds to the real part of Z_{elec}. The vibratory component X_E corresponds to the imaginary part of Z_{elec}.

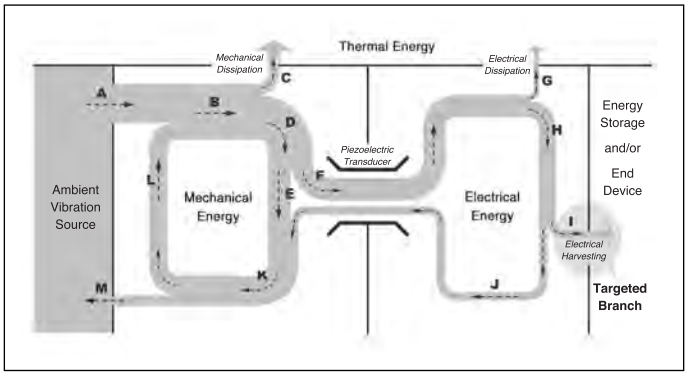

Figure 6 – Energy Flow Chart

In SEH, the electrical dissipation is attributed to the forward voltage drop of the rectifier V_F. The three components in Z_{elec} can be calculated as follows:

$$R_d = \frac{4}{\pi\omega C_p}\tilde{V}_F(1-\tilde{V}_{rect}) \tag{8}$$

$$R_h = \frac{4}{\pi\omega C_p}(\tilde{V}_{rect}-\tilde{V}_F)(1-\tilde{V}_{rect}) \tag{9}$$

$$X_E = \frac{1}{\pi\omega C_p}(\sin\theta\cos\theta-\theta) \tag{10}$$

All of the three component values are functions of $\tilde{V}_{rect}$. With the quantitative analysis on the detailed composition in Z_{elec}, the equivalent circuit given in Fig 3 can be further derived into the equivalent impedance network, as shown in Fig 7. X_L and X_C are the corresponding reactances of L and C in Fig 3 respectively. The real components are represented by gray blocks, while the imaginary ones are represented by white blocks. The three components of R_d, R_h and X_E are variables (denoted with arrows), which are functions of the non-dimensional rectified voltage $\tilde{V}_{rect}$ (denoted with dashed lines linking to $\tilde{V}_{rect}$).

In the equivalent impedance network, all of the real components extract power from the system; yet, the function of the harvesting component R_h is different from those of the dissipative component R and R_d. In order to distinguish the functional difference, R_h is marked with the recycling symbol. Since the harvested power is the target in the optimisation, with the conventional concept about source and load impedances, the harvesting component R_h should be regarded as the 'load impedance'; the rest components in the network, ie X_L, R, X_C, X_E, and R_d form the 'source impedance'.

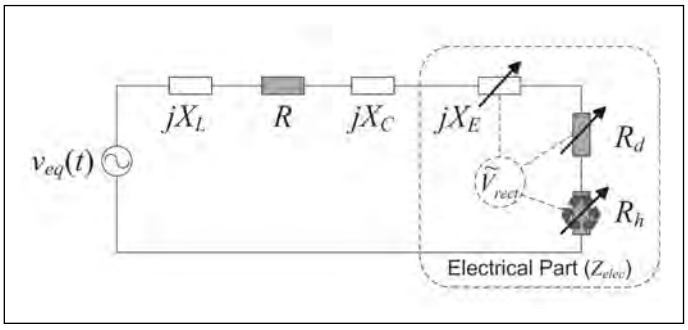

Figure 7 – Equivalent Impedance Network of a Base Excited PEH Device

Harvested Power Optimisation

In the previous section, the equivalent impedance network of a PEH system was proposed based on the clarifications on the four issues, which were overlooked previously. With the new understandings, the harvested power optimisation issue can be further investigated.

Conventional Impedance Matching

The conventional impedance matching theory was originally proposed for series impedance network driven by a voltage source or parallel impedance network driven by a current source. Since the equivalent impedance network of the PEH system is a series impedance network driven by a voltage source, Fig 8 shows the conventional series impedance network for comparison. In the conventional impedance network, the magnitude of source voltage is fixed; the source impedance is a fixed complex number. If the load impedance is an arbitrary complex number, the maximum load power is attained when the load impedance is the complex conjugate of the source impedance, ie:

$$Z_{load} = Z^*_{source} \tag{11}$$

On the other hand, if the load impedance is confined as an arbitrary real number, ie resistive load, the load power is maximised when the load impedance equals the magnitude of the source impedance, ie:

$$Z_{load} = |Z_{source}| \tag{12}$$

Both of these two criteria were discussed for the harvested power optimisation in PEH systems (Brufau-Penella and Puig-Vidal, 2009; Kong *et al.*, 2010). Nevertheless, the differences between the PEH systems and the conventional impedance network did not receive enough attention.

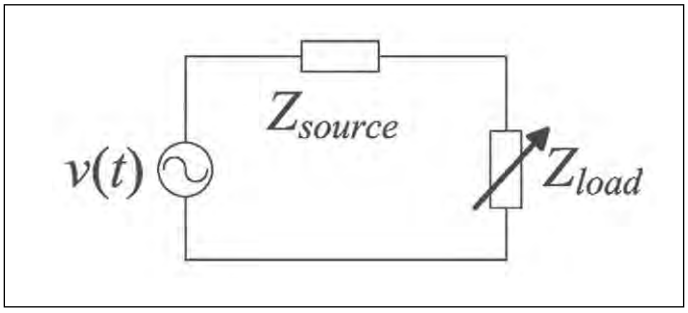

Figure 8 – Conventional Series Impedance Network with a Voltage Source

Constrained Impedance Matching in PEH Systems

Comparing the equivalent impedance network shown in Fig 7 (X_L, R, X_C, X_E, and R_d form the 'source impedance' and R_h is the 'load impedance') to the conventional impedance network shown in Fig 8, two distinctions are observed:

1) The 'source impedance' in the PEH equivalent impedance network is variable, and its value changes with the 'load impedance';
2) The 'load impedance' in the PEH network is purely resistive, but its value is constrained, rather than arbitrary.

Taking these two differences into consideration, neither the conventional complex conjugate impedance matching nor the resistive impedance matching is applicable for the harvested power optimisation in the PEH systems. The harvested power can be calculated with the equivalent impedance network shown in Fig 7:

$$P_h = \frac{V_{eq}^2}{2} \frac{R_h}{(X_L + X_C + X_E)^2 + (R + R_d + R_h)^2} \tag{13}$$

where V_{eq} is the magnitude of the equivalent voltage source v_{eq}. Given that X_E, R_d and R_h are variables depending on the non-dimensional rectified voltage $\tilde{V}_{rect}$, the harvested power optimisation problem can be expressed with the following expression:

$$\max \frac{R_h}{(X_L + X_C + X_E)^2 + (R + R_d + R_h)^2} \tag{14}$$

s.t. the constraints of R_d, R_h, and X_E.

The closed form expression would be difficult to obtain. The problem can be solved with a numerical searching method.

The Matching Index

The load impedance in the equivalent impedance network of a PEH system, ie R_h, is resistive. In the resistive impedance matching, maximum load power is obtained when Eqn (12) is satisfied. In the equivalent impedance network of PEH systems, the ratio between R_h and $|Z_{source}|$ is defined as the matching index:

$$\lambda = \frac{R_h}{|Z_{source}|} = \frac{R_h}{\sqrt{(X_L + X_C + X_E)^2 + (R + R_d)^2}} \tag{15}$$

λ represents the relation between the load and source impedances. In the conventional resistive matching point, λ equals one. But in the PEH system, it is not necessary that the closer between λ and one, the more power can be delivered to R_h, because the source impedance is not fixed. Therefore, λ can only be used to show the relation between the load and source here. In a weakly coupled PEH device, R_h is usually much smaller than $|Z_{source}|$; therefore, $\lambda << 1$.

Experiment

To verify the constrained impedance matching for harvested power optimisation, experiments are carried out on a base excited PEH system with the SEH interface circuit connected. The experimental setup is shown in Fig 9(a). The piezoelectric patch is attached near the fixed end of an aluminium cantilever, which is excited by a 46 Hz harmonic base excitation. This harmonic excitation is provided by an electromagnetic shaker in experiment. In practical applications, the vibration could be from vibrating machines, eg engines. Therefore, the fundamental natural frequency of the PEH device could be tuned to match the frequency of the vibration source. Before applying the vibration, the internal impedance of the piezoelectric structure is measured with an impedance analyser (4294A, Agilent). The measured result (magnitude and phase) is shown in Fig 9(b). The parameters of L, C, R, and C_p are identified with the process of fitting the measured curves. The values of these parameters as well as the first mode resonant frequency f_0 are listed in Table 2.

Given the C_p value in Table 2 and based on Eqn (8) to Eqn (10), the three components in the electrical part, ie R_d, R_h and X_E, can be specified as

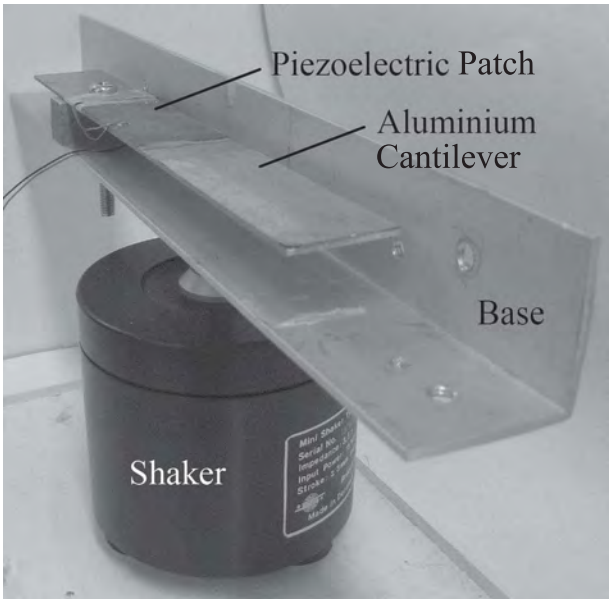

(a) Experimental Setup

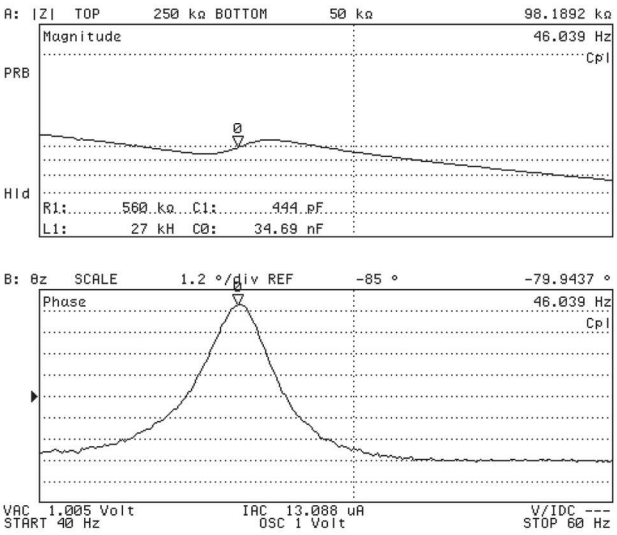

(b) Impedance Magnitude and Phase

Figure 9 – Experimental Setup and Measured Impedance

Component	Value
L	27 kH
C	444 pF
R	560 kΩ
C_p	34.69 nF
f_0	46.039 Hz
V_F	1.0 V

Table 2 – Parameters of Experimental Setup

functions of $\tilde{V}_{rect}$. With all the obtained parameters, the harvested power can be theoretically calculated with Eqn (13). Experiments are carried out for validation. Different dc load resistors are connected one after another to stabilise the rectified voltage at different level. The corresponding experimental result on the harvested power is:

$$P_{h,exp} = \frac{V_{store}^2}{R_{load}} \tag{16}$$

Fig 10 shows that the theoretical and experimental results agree quite well under three $\tilde{V}_F$ conditions. It is also shown that the optimal $\tilde{V}_{rect}$ (corresponding to the maximum P_h) changes with $\tilde{V}_F$. The optimal point of $\tilde{V}_{rect}$ under different $\tilde{V}_F$ moves along the solid curve in Fig 10.

To have more insights about the relation between the mechanical and electrical equivalent impedances in the experiment, Fig 11 illustrates the mechanical equivalent impedance as well as the available electrical equivalent impedance in the complex impedance plane. It has been shown

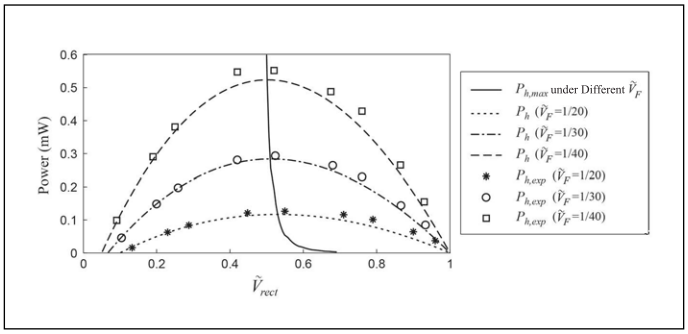

Figure 10 – Harvested Power as Functions of Rectified Voltage $\tilde{V}_{rect}$

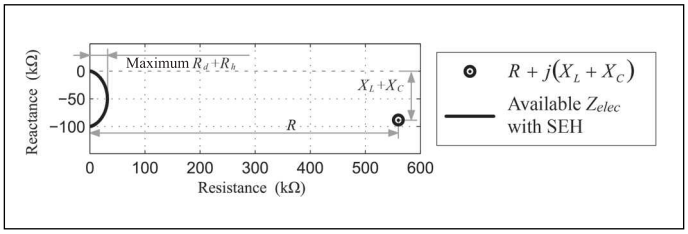

Figure 11 – Equivalent Impedance of the Mechanical and Electrical Parts

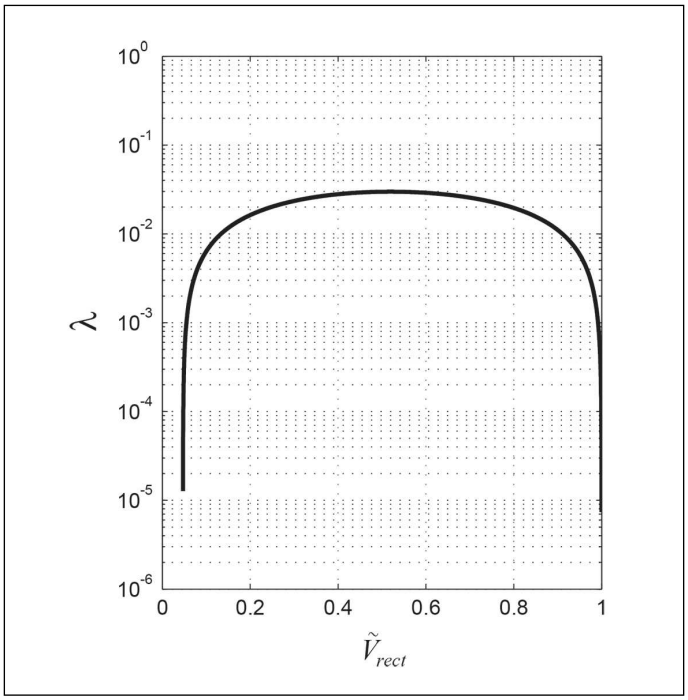

Figure 12 – Matching Index in the PEH Experiment

that the maximum $R_h + R_d$ is much smaller than R. Under resonance ($X_L + X_C + X_E = 0$), the majority of loss power is consumed by the mechanical dissipation, rather than electrical dissipation or electrical harvesting.

The relation between the equivalent source and load impedances in the PEH system is reflected by the matching index λ defined in Eqn (15). Fig 12 shows λ as a function of the non-dimensional rectified voltage $\tilde{V}_{rect}$. As observed from Fig 12, the maximum value of λ in this given system is about 0.03, which is much smaller than one. The value of R_h is not comparable to the magnitude of the source impedance. Therefore, the constrained impedance matching in the PEH systems is very different from the unconstrained impedance matching in the conventional impedance network.

Conclusion

The harvested power optimisation in the piezoelectric energy harvesting (PEH) systems was investigated from the impedance matching point of view. Even this topic was discussed in some of the previous literature, four fundamental issues were not thoroughly considered or even misunderstood. Restarting from the origin of the impedance matching theory, the equivalent impedance network of the PEH system was proposed and investigated in this paper. The scope of the impedance network, the definition, available range and detailed composition of the electrical part equivalent impedance were comprehensively studied. Based on these fundamental understandings, the distinctions between the equivalent impedance network of a PEH system and the conventional impedance network were pointed out. Rather than directly using the complex conjugate or resistive impedance matching criteria as the previous literature did, constrained impedance matching was adopted for the harvested power optimisation in PEH systems. Experiments showed that the harvested power can be well predicted by the equivalent impedance network, and the maximum point of the harvested power can be accurately estimated.

Acknowledgements

The work described in this paper was fully supported by a grant from the Research Grants Council of the Hong Kong Special Administrative Region, China (Project No CUHK 414809).

References

1. Beeby, S.P., Tudor, M.J., White, N.M., Energy harvesting vibration sources for microsystems applications. *Measurement Science and Technology*. Volume 17, No 12, pp R175-R195. Institute of Physics. UK (2006).
2. Brufau-Penella, J., Puig-Vidal, M., Piezoelectric energy harvesting improvement with complex conjugate impedance matching. *Journal of Intelligent Material Systems and Structures.* Volume 20, No 5, pp597-608. Sage Publications. UK (2009).
3. Cook-Chennault, K.A., Thambi, N., Sastry, A.M., Powering MEMS portable devices - a review of non-regenerative and regenerative power supply systems with special emphasis on piezoelectric energy harvesting systems. *Smart Materials and Structures*. Volume 17, No 4, p043001. Institute of Physics. UK (2008).
4. Elvin, N.G., Elvin, A.A., A general equivalent circuit model for piezoelectric generators. *Journal of Intelligent Material Systems and Structures*. Volume 20, No 1, pp3-9. Sage Publications. UK (2009).
5. Guan, M.J., Liao, W.H., On the equivalent circuit models of piezoelectric ceramics. *Ferroelectrics*. Volume 386, No 1, pp77-87. Taylor & Francis. UK (2009).
6. Hudak, N.S., Amatucci, G.G., Small-scale energy harvesting through thermoelectric, vibration, and radiofrequency power conversion. *Journal of Applied Physics*. Volume 103, No 10, p101301. American Institute of Physics. USA (2008).
7. Kim, H., Priya, S., Stephanou, H., Uchino, K., Consideration of impedance matching techniques for efficient piezoelectric energy harvesting. *IEEE Transactions on Ultrasonics, Ferroelectrics, and Frequency Control*. Volume 54, No 9, pp1851-1859. Institute of Electrical and Electronics Engineers. USA (2007).
8. Kong, N., Ha, D.S., Erturk, A., Inman, D.J., Resistive impedance matching circuit for piezoelectric energy harvesting. *Journal of Intelligent Material Systems and Structures.* Volume 21, No 13, pp1293-1302. Sage Publications. UK (2010).

9. Liang, J.R., Liao, W.H., Piezoelectric energy harvesting and dissipation on structural damping. *Journal of Intelligent Material Systems and Structures.* Volume 20, No 5, pp515-527. Sage Publications. UK (2009).
10. Liang, J.R., Liao, W.H., Energy flow in piezoelectric energy harvesting systems. *Smart Materials and Structures*. Volume 20, No 1, p015005. Institute of Physics. UK (2011).
11. Rodig, T., Schonecker, A., Gerlach, G.A., Survey on piezoelectric ceramics for generator applications. *Journal of the American Ceramic Society*. Volume 93, No 4, pp901-912. American Ceramic Society. USA (2010).
12. Scruggs, J., On the causal power generation limit for a vibratory energy harvester in broadband stochastic response. *Journal of Intelligent Material Systems and Structures.* Volume 21, No 13, pp1249-1262. Sage Publications. UK (2010).
13. Stephen, N., On the maximum power transfer theorem within electromechanical systems. *Proceedings of the Institution of Mechanical Engineers, Part C: Journal of Mechanical Engineering Science*. Volume 220, No 8, pp1261-1267. Sage Publications. UK (2006).
14. Stephen, N., On energy harvesting from ambient vibration. *Journal of Sound and Vibration.* Volume 293, No 1-2, pp409-425. Elsevier. Netherlands (2006).
15. Uchino, K., Ishii, T., Energy flow analysis in piezoelectric energy harvesting systems. *Ferroelectrics*. Volume 400, No 1, pp305-320. Taylor & Francis. UK (2010).
16. Yang, Y., Tang, L., Equivalent circuit modelling of piezoelectric energy harvesters. *Journal of Intelligent Material Systems and Structures*. Volume 20, No 18, pp2223-2235. Sage Publications. UK (2009).

About the Authors

LIANG Junrui **PhD MIEEE MASME**
Email: jrliang@cuhk.edu.hk

Dr Liang received his BEng and MEng degrees in instrumentation engineering from Shanghai Jiao Tong University, Shanghai, China, in 2004 and 2007, respectively, and the PhD degree in mechanical and automation engineering from The Chinese University of Hong Kong, Hong Kong, China, in 2010. He is now a Postdoctoral Fellow in The Chinese University of Hong Kong. His research interests include piezoelectric devices, energy harvesting, and Class-E power amplifiers. Dr Liang is a recipient of two Best Paper Awards and one Best Student Contributions Award in three international conferences.

LIAO Wei Hsin **PhD FASME FInstP**
Email: whliao@cuhk.edu.hk

Dr Liao is a Professor at the Department of Mechanical and Automation Engineering, The Chinese University of Hong Kong. His research has led to publications of over 130 technical papers, 5 patents and 4 other patent applications. Two of the journal papers he coauthored were awarded by the Institution of Mechanical Engineers, and the American Society of Mechanical Engineers, respectively. He is also a recipient of four Best Paper Awards in IEEE conferences. Dr Liao is an Associate Editor for ASME Journal of Vibration and Acoustics, Journal of Intelligent Material Systems and Structures, as well as Smart Materials and Structures.